Autumnal bottom-up and top-down impacts of Cyanea capillata: a mesocosm study

Journal of
Plankton Research

plankt.oxfordjournals.org

J. Plankton Res. (2015) 37(5): 1042–1055. First published online June 17, 2015 doi:10.1093/plankt/fbv046

Contribution to the ICES/PICES Theme Session: 'Interactions of Gelatinous Zooplankton within Marine Food Webs'

Autumnal bottom-up and top-down impacts of *Cyanea capillata*: a mesocosm study

AINO HOSIA[1†]*, CHRISTINA B. AUGUSTIN[2‡], JULIE DINASQUET[3¶], LENA GRANHAG[4], MARIA L. PAULSEN[5], LASSE RIEMANN[3], JANNE-MARKUS RINTALA[6,7], OUTI SETÄLÄ[8], JULIA TALVITIE[9] AND JOSEFIN TITELMAN[10]

[1]INSTITUTE OF MARINE RESEARCH, BERGEN N-5817, NORWAY, [2]BIOLOGICAL OCEANOGRAPHY, LEIBNIZ INSTITUTE FOR BALTIC SEA RESEARCH WARNEMÜNDE, ROSTOCK D-18119, GERMANY, [3]MARINE BIOLOGICAL SECTION, UNIVERSITY OF COPENHAGEN, HELSINGØR DK-3000, DENMARK, [4]DEPARTMENT OF SHIPPING AND MARINE TECHNOLOGY, CHALMERS UNIVERSITY OF TECHNOLOGY, GOTHENBURG SE-41296, SWEDEN, [5]DEPARTMENT OF BIOLOGY, DEPARTMENT OF MARINE MICROBIOLOGY, UNIVERSITY OF BERGEN, BERGEN N-5006, NORWAY, [6]DEPARTMENT OF ENVIRONMENTAL SCIENCES, UNIVERSITY OF HELSINKI, HELSINKI FI-00014, FINLAND, [7]TVÄRMINNE ZOOLOGICAL STATION, UNIVERSITY OF HELSINKI, HANKO FI-10900, FINLAND, [8]SYKE MARINE RESEARCH CENTRE, HELSINKI FI-00251, FINLAND, [9]DEPARTMENT OF CIVIL AND ENVIRONMENTAL ENGINEERING, AALTO UNIVERSITY, ESPOO FI-02150, FINLAND AND [10]DEPARTMENT OF BIOSCIENCES, UNIVERSITY OF OSLO, P.O. BOX 1066 BLINDERN, OSLO N-0316, NORWAY

[†]PRESENT ADDRESS: UNIVERSITY MUSEUM OF BERGEN, DEPARTMENT OF NATURAL HISTORY, BERGEN N-5007, NORWAY.
[‡]PRESENT ADDRESS: AQUACULTURE AND SEA-RANCHING, FACULTY OF AGRICULTURAL AND ENVIRONMENTAL SCIENCES, UNIVERSITY OF ROSTOCK, ROSTOCK D-18059, GERMANY.
[¶]PRESENT ADDRESS: DIVISION OF MARINE BIOLOGY RESEARCH, SCRIPPS INSTITUTION OF OCEANOGRAPHY, UCSD, LA JOLLA, CA, USA.

*CORRESPONDING AUTHOR: aino.hosia@gmail.com

Received December 12, 2014; accepted May 25, 2015

Corresponding editor: Marja Koski

Jellyfish are effective predators on mesozooplankton and release large amounts of dissolved organic matter. Nevertheless, jellyfish initiated trophic cascades and bottom-up influences impacting lower trophic levels have received limited attention. We conducted a mesocosm experiment to quantify simultaneous top-down and bottom-up effects of a common jellyfish, *Cyanea capillata*, in a natural plankton community during autumn. Treatments were 0, 2 or 5 jellyfish per 2.5 m^3 mesocosm, four replicates each, with initial additions of inorganic nutrients. Primary and bacterial production, species abundance and composition of several trophic levels and nutrient and carbon dynamics were followed during the 8-day experiment. Multivariate statistics and generalized additive mixed modelling were applied to test whether jellyfish carbon concentration (0–1.26 mg *jellyC* L^{-1}) in the mesocosms affected the variables monitored. Unexpected negligible predatory impact of jellyfish on mesozooplankton was observed, potentially related to jellyfish senescence. Community compositions of bacteria, phytoplankton and mesozooplankton changed with time, but did not differ between treatments. However, nutrient regeneration by jellyfish was evident, and jellyfish had

available online at www.plankt.oxfordjournals.org

a positive impact on total and specific bacterial production, total primary production and the >10 μm chlorophyll *a* fraction. Bottom-up influences from abundant jellyfish could thus stimulate productivity in nutrient depleted autumnal surface waters.

KEYWORDS: gelatinous zooplankton; trophic interactions; food web; trophodynamics; productivity

INTRODUCTION

Jellyfish are ubiquitous components of marine zooplankton and can at times occur in great numbers forming blooms or aggregations. Abundant jellyfish can considerably impact pelagic cycling of carbon and nutrients through both top-down and bottom-up processes. Many jellyfish are voracious predators on mesozooplankton and ichthyoplankton, and can initiate trophic cascades affecting even lower trophic levels (Verity and Smetacek, 1996; Granéli and Turner, 2002; Stibor *et al.*, 2004; West *et al.*, 2009a; Dinasquet *et al.*, 2012a; McNamara *et al.*, 2014). While the bottom-up influences of jellyfish have been less studied, the release of organic carbon and cycling of nutrients by jellyfish can impact both bacterial and primary production (Hansson and Norrman, 1995; Riemann *et al.*, 2006; Pitt *et al.*, 2009; Dinasquet *et al.*, 2012b). In addition to redirecting the flow of carbon from fish to jellyfish, abundant jellyfish may alter the composition and functioning of the microbial community (Dinasquet *et al.*, 2013), potentially resulting in increased removal of carbon from the system via bacterial respiration due to decreased growth efficiency of bacteria consuming dissolved organic matter (DOM) originating from jellyfish (Condon *et al.*, 2011). Post bloom, jellyfish carcasses sink rapidly, contributing to the vertical flux of organic matter and sequestration of carbon by the oceans (Lebrato *et al.*, 2013), while also leaking considerable amounts of organic matter and nutrients, thus affecting the microbial community and increasing oxygen demand (Titelman *et al.*, 2006; West *et al.*, 2009b; Tinta *et al.*, 2010; Frost *et al.*, 2012).

It has been suggested that anthropogenic drivers, such as fisheries and habitat modification, climate change and environmental degradation resulting in eutrophication, hypoxia and reduced optical conditions, may be contributing towards increased jellyfish abundances and more frequent blooms, at least locally, with potential negative consequences for, e.g. fisheries, tourism, industry and recreational activities (reviewed in Purcell *et al.*, 2007). Nevertheless, studies addressing the ecological effects of jellyfish apart from their direct predatory impact remain scarce, and jellyfish are frequently treated as insignificant trophic dead-ends or ignored in food web models. Only a handful of mesocosm studies looking at the combined top-down and bottom-up impacts of gelatinous predators have so far been conducted (but see Granéli and Turner, 2002; West *et al.*, 2009a, b; Dinasquet *et al.*, 2012a; McNamara *et al.*, 2014).

Cyanea capillata is a common cold-water scyphozoan with a circumpolar distribution in the North Atlantic (Russell, 1970). It is seasonally abundant along the entire Norwegian coast; in southern Norway, it typically appears in the spring, peaks around June, and declines through autumn to disappear in November–December (Hosia *et al.*, 2014). *Cyanea capillata* feeds readily on both mesozooplankton and other gelatinous zooplankters both under natural conditions and in captivity (Båmstedt *et al.*, 1994; Martinussen and Båmstedt, 1995; Titelman *et al.*, 2007; Hosia and Titelman, 2011). While the diet and feeding rates of *C. capillata* in Scandinavian waters have received attention, their potential role in initiating trophic cascades and their bottom-up effects are largely unexplored. Here, we used a mesocosm approach to identify and quantify simultaneous top-down and bottom-up effects of these jellyfish across all trophic levels of a natural plankton community, in an effort to better understand their overall impact in the pelagic ecosystem.

METHOD

Experimental set-up and sampling

The experiment was carried out 1–8 October 2011 at the outdoor land-based mesocosm facility of Espegrend Marine Biological Station (University of Bergen), located by Raunefjord at ~60.27°N, 5.22°E. Twelve cylindrical 2.5 m^3 (~1.5 m diameter and height) white fibreglass mesocosms were used. The mesocosms were exposed to natural light and to reduce daily temperature fluctuations, they were placed within larger cylindrical tanks with continuous flow-through of Raunefjord water from 40 m depth. The day before the experiment started, the mesocosms were washed and filled with Raunefjord water pumped from ~10 m depth. Filling was done sequentially, one-third at a time, to ensure similar start conditions in all mesocosms.

To avoid nutrient limitation (cf. Dinasquet *et al.*, 2012a), nutrients (8 μM nitrate as $NaNO_3$, 0.5 μM phosphate as KH_2PO_4 and 24 μM silicate as $Na_2SiO_3 \cdot 5H_2O$) were added to each mesocosm the day before the experiment started. Non-filtering pond pumps and PVC tubing were used to create continuous circulation from the surface to

the bottom (mean flow rate 9.1 L min^{-1}) in a manner that prevented jellies from getting caught in the suction.

Cyanea capillata were gently collected with buckets from the surface of Raunefjord the day before the experiment began, and kept in several ~2.5 m^3 holding tanks overnight. The experiment commenced on 1 October (Day 1), when jellyfish were added to the mesocosms, followed immediately by the first sampling. Three treatments with four replicates each were set up: controls without jellyfish, a low-density treatment with two jellyfish, and a high-density treatment with five jellyfish per mesocosm (Fig. 1). The highest resulting jellyfish carbon concentrations compared realistically to extreme natural blooms (Lucas *et al.*, 2014). All jellyfish were intact and active at the start and were monitored each morning for vitality. After final sampling on Day 8, the jellyfish were removed, measured for wet weight and bell diameter, and inspected for damage and planula larvae. Jellyfish carbon content (Y, mg C) was calculated from their diameter (d, cm) as $Y = 0.673d^{2.788}$ (Martinussen and Båmstedt, 1995).

Mesocosms were sampled daily; in the afternoon on Day 1, and in the morning on the subsequent days. A vertically integrated 5 L sample was taken from each mesocosm with an acrylic sampling tube and transferred to an HDPE container with tap. The containers were placed in a temperature-controlled room (~14°C) and subsamples for the monitored parameters were drawn from these immediately (Table I). Temperature, salinity and oxygen were measured daily directly from the mesocosms with a Cond 3110 (WTW) conductivity metre and an Oxi 3205 (WTW) oximeter. In addition, a DST CTD (Star Oddi) continuously monitored temperature and salinity in one of the mesocosms.

Carbon, nutrients and chlorophyll *a*

To minimize gas exchange, dissolved inorganic carbon (DIC) was always the first sample to be drawn from the 5-L containers. DIC samples were preserved with $HgCl_2$, sealed and stored refrigerated in the dark. The samples were analysed by coulometric titration of the gas extracted from the sample acidified with phosphoric acid, using a VINDTA system (MARIANDA), modelled after the SOMMA system (Johnson *et al.*, 1985), following the standard operating procedure of Dickson *et al.* (Dickson *et al.*, 2007). Certified Reference Material from Dr A. G. Dickson, Scripps Institution of Oceanography, was routinely measured to assure accuracy and precision (± 2 μmol kg^{-1}). Since the DIC samples taken on Days 1, 2, 3, 5 and 8 (2014.19 ± 53.69, mean and SD) showed a consistent linear decrease over time in all mesocosms (β −25.6 ± 1.5, mean and SD, and $r^2 \geq 0.99$ for all mesocosms), the missing days were separately interpolated for each mesocosm for the primary production calculations.

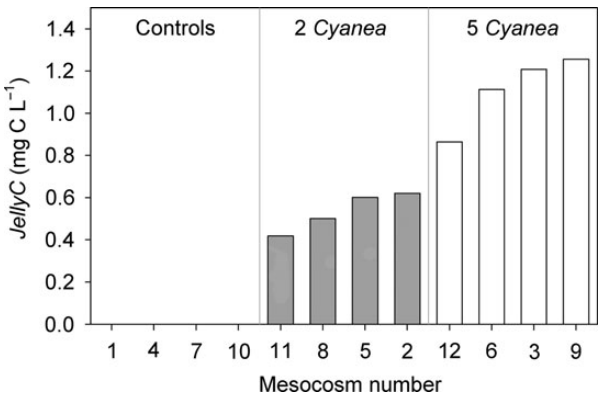

Fig. 1. Jellyfish carbon (*JellyC*) in mesocosms and treatments.

Total organic carbon (TOC) samples were fixed with phosphoric acid and stored refrigerated in the dark. TOC was determined with a Torch Combustion TOC Analyser (Teledyne Tekmar), calibrated with distilled water blanks and potassium hydrogen phthalate standards. Samples for particulate organic carbon (POC) and nitrogen (PON) were filtered on pre-combusted GF/F filters and frozen at −20°C in pre-combusted test tubes. POC and PON samples were prepared for analysis following Grasshof *et al.* (Grasshof *et al.*, 1983) and measured using a Thermo Finnegan Flash EA 1112 element analyser. Dissolved organic carbon (DOC) was calculated as the difference between TOC and POC.

Ammonium (NH_4^+) samples were frozen at −20°C and later measured fluorometrically with an Alpkem Flow Solution IV autoanalyser. Samples for inorganic nutrients (NO_3^-, NO_2^-, PO_4^{3-} and SiO_4^{4-}) were fixed with chloroform, stored refrigerated in the dark and later measured spectrophotometrically with an Alpkem Flow Solution IV or modified Skalar autoanalyser.

Chlorophyll *a* (chl *a*) samples were filtered on both Munktell MGF filters (total chl *a*) and 10 μm Whatman Nuclepore filters (>10 μm fraction) and stored at −20°C. Pigments were extracted with 90% acetone and determined fluorometrically using a Turner Designs Model 10-AU-005 field fluorometer.

Apart from DIC and TOC, all samples above were collected according to the standard protocols of and analysed by the accredited inorganic chemistry laboratory at the Institute of Marine Research, Bergen, Norway (Norwegian Accreditation, accr.no. TEST 166).

Primary production

Primary production was measured using the ^{14}C method (Steemann Nielsen, 1952) modified by Niemi *et al.* (Niemi

Table I: List over sampled parameters, sampling frequency and the number of mesocosms sampled per sampling event

Sampled parameter	Sampling frequency	*N* mesocosms
Ammonium	Daily	12
Bacterial abundance	Daily	12
Bacterial community	Daily (Days 1, 3, 5, 7, 8 analysed)	6 (2 per treatment)
Bacterial production	Daily	12
Chlorophyll *a*, >10 μm	Daily	12
Chlorophyll *a*, total	Daily	12
Ciliates	Daily (Days 1, 2, 6, 8 counted)	12
Dissolved inorganic carbon (DIC)	Days 1, 2, 3, 5, 8	12
Heterotrophic nanoflagellates	Daily (Days 1, 2, 5, 7, 8 counted)	12 (2 in Day 1)
Mesozooplankton	Start and end	12 (for end)
Nitrate	Daily	12
Nitrite	Daily	12
Oxygen	Daily	12
Particulate organic carbon (POC)	Daily	12
Particulate organic nitrogen (PON)	Daily	12
Phosphate	Daily	12
Phytoplankton community	Daily (Days 1, 4, 8 counted)	12
Primary production	Daily	12
Salinity	Daily	12
Silicate	Daily	12
Small autotrophs with FCM	Daily	12
Temperature	Daily	12
Temperature and salinity with DST CTD	Continuous	1
Total organic carbon (TOC)	Daily (Days 2–8 analysed)	12
Viruses	Daily	12

Note that for mesozooplankton, common start samples for all mesocosms were taken in between the sequential filling of the containers. Occasional missing samples are not accounted for—see Table II for total no. of samples analysed.

et al., 1983). $NaH_{14}CO_3$ (specific activity 20 μ Ci mL^{-1}, C14 Centralen, DK; final concentration 0.05 μ Ci mL^{-1}) was added to three 50 mL subsamples from each treatment, the sterile tissue culture flasks were immediately closed and one parallel was covered with aluminium foil as a dark control. Bottles were incubated in clear plastic bags on the surface of a mesocosm for 24 h. Incubations were stopped by adding 200 μL formaldehyde. From each sample, 4 mL was acidified with 100 μL 1 N HCL in a glass scintillation bottle, kept open in a fume hood for 24 h to remove unincorporated $NaH_{14}CO_3$. InstaGel Plus (PerkinElmer) scintillation cocktail was added to the acidified samples and the activity was measured with Wallac WinSpectral 1414 liquid scintillation counter. The difference between dark and light treated bottles was converted into *in situ* estimates of primary production (μg C L^{-1} h^{-1}) taking into account the DIC present. For primary production per unit biomass, these estimates were normalized relative to chl *a*.

Viruses, bacteria and small autotrophs

Samples for abundances of bacteria, viruses and small autotrophs were fixed with 0.2 μm filtered 25% glutaraldehyde (final conc. 0.5%), kept in the dark at 4°C for 20 min, flash frozen in liquid nitrogen and stored at −80°C until analysis with a FACS Calibur (Beckton Dickinson) flow cytometer. Thawed samples for bacteria and virus enumeration were diluted 100-fold in 0.2-μm filtered TE buffer (Tris 10 mM, EDTA 1 mM, pH 8), stained with SYBR Green I (Molecular Probes, Inc., Eugene, OR, USA) and incubated for 10 min at 80°C (Marie *et al.*, 1999). Abundances of low (LNA) and high (HNA) nucleic acid bacteria and viruses were distinguished as in Huete-Stauffer and Morán (Huete-Stauffer and Morán, 2012). Samples for small autotrophs were analysed directly after thawing and groups of unidentified picoeukaryotes, picoprokaryotes (*Synechococcus*), unidentified nanophytoplankton, *Emiliania huxleyi* and cryptophytes were discriminated on the basis of their side scatter, chl *a* (red) and phycoerythrin (orange) fluorescence as in Bratbak *et al.* (Bratbak *et al.*, 2011). Flow cytometric data were processed using CellQuest software and cell numbers were calculated from the instrument flow rate based on volumetric measurements about every 4 h.

Bacterial production

Bacterial production was measured by the 3H-thymidine incorporation method as in Smith and Azam (Smith and Azam, 1992). Triplicate 1.5 mL subsamples and single trichloroacetic acid killed controls were incubated in polypropylene tubes with 16 nM (final concentration)

3H-thymidine (84.5 Ci mmol^{-1}, PerkinElmer) in the dark, on the surface of a mesocosm for 1 h. Incubations were stopped by adding 89 μL of ice cold 100% TCA. Samples were centrifuged at 16 000 g and +4°C for 10 min and washed once with refrigerated 5% TCA and once with 80% ethanol. After washing, 0.5 mL of InstaGel Plus (PerkinElmer) scintillation cocktail was added to the samples and shaken well to dissolve the pellet. After initial storage at room temperature, the samples were refrigerated until measuring of radioactivity with a Wallac WinSpectral 1414 liquid scintillation counter. Thymidine incorporation was converted to carbon production using conversion factor of 1.1×10^{18} cells mol^{-1} (Riemann *et al.*, 1987). The bacterial cell volumes were assumed to be 0.13 μm^3 (Tuomi *et al.*, 1995) and volumes were converted to carbon biomass by multiplying by 0.22 g of C cm^{-3} (Bratbak and Dundas, 1984).

Bacterial community composition

For bacterial community composition, ~1 L of sample water was filtered onto a 0.2-μm Supor filter (Pall Life Sciences) and frozen at −80°C. DNA was extracted using an enzyme/phenol-chloroform protocol (Riemann *et al.*, 2000) but with a 30-min lysozyme digestion at 37°C and an overnight proteinase K digestion (20 mg mL^{-1} final conc.) at 55°C (Boström *et al.*, 2004). Bacterial 16S rRNA genes were PCR amplified, purified and sequenced as in (Dinasquet *et al.*, 2012b). The samples were mixed in equimolar amounts and sequenced from the reverse primer direction using Roche/454 GS FLX Titanium technology (National High-throughput DNA Sequencing Centre, University of Copenhagen).

Sequences were processed with Quantitative Insights Into Microbial Ecology software (QIIME v1.3, (Caporaso *et al.*, 2010) as described in Dinasquet *et al.* (Dinasquet *et al.* 2012b). The phylogenetic similarity between samples was determined by principal component analysis (PCA) using weighted-UniFrac distances within QIIME between randomly picked OTUs (normalized to 2618 sequences per sample to accommodate for the lowest number of sequences found in a sample). All sequences obtained in this study have been deposited in the European Nucleotide Archive−Short Read Archive under the accession number PRJEB7907.

Heterotrophic nanoflagellates and ciliates

Heterotrophic nanoflagellate (HNF) samples were preserved with 0.2-μm filtered 25% glutaraldehyde (final conc. 1.25%). For counts, 5 mL subsamples were stained with proflavine, filtered onto 0.2-μm polycarbonate filters, mounted in paraffin oil on slides and frozen (Kuuppo-Leinikki and Kuosa, 1989). Flagellates were counted in at least 50 fields from each filter with an epifluorescence microscope (Leica Aristoplan) under blue excitation light.

Ciliate samples were fixed with acid Lugol's solution (final conc. 1−2%) and counted from 25 to 50 mL settled samples (Utermöhl, 1958) using an inverted microscope (Leica DMIL, ×100−400 magnifications).

HNF and ciliate samples were not counted for all days, with the total number of samples included in the analyses being 45 and 55, respectively (Tables I and II).

Phytoplankton and mesozooplankton

Phytoplankton samples were preserved in neutral Lugol's solution (final conc. ~1%) and algal cells were identified and enumerated for Days 1, 4 and 8 in a 0.1-mL P-M cell (detection limit 10 000 cell L^{-1}). For larger, less abundant species, 25 mL of the sample was filtered onto a semi-transparent membrane filter (Metricel PALL GN-6, 0.45 μm) and the phytoplankton on the filter identified and enumerated (detection limit 40 cell L^{-1}).

The water used for filling the mesocosms was not filtered apart from a coarse sieve to remove large animals and detritus, thus retaining the natural plankton community. Start samples for mesozooplankton ($n = 5$) were taken with a 90-μm net in between the sequential filling of the mesocosms. To avoid serial depletion, no mesozooplankton samples were taken during the experiment. At the end of the experiment, the water from each mesocosm was filtered through a 90-μm plankton net to obtain end samples. These were preserved in 10% borax-buffered formalin and mesozooplankton were identified and enumerated under a stereomicroscope.

Statistical methods

Permutational multivariate analysis of variance (PERMANOVA: function *adonis* in R package *vegan*; Oksanen *et al.*, 2013) was used to test for differences in community composition of mesozooplankton and phytoplankton. Abundances were $\log(x + 1)$ transformed prior to analysis. Differences in community composition were visualized with non-metric multidimensional scaling plots using Bray-Curtis distances.

Since start conditions in all mesocosms were assumed to be equal, the only known difference between them was the addition of varying amounts of jellyfish. We set up three treatments with four replicates each, but converting the jellyfish diameters to carbon content revealed a series of jellyfish carbon (*JellyC*) concentrations (Fig. 1). We therefore applied generalized additive mixed modelling (GAMM; function *gamm*, R package *mgcv*; Wood, 2011) to test for effects of *JellyC* on each response variable

Table II: Summary of results from GAMM. Response variables modelled with negative binomial distribution and log link (Model 2, see text for details) are marked with NB in the Adjustments column, with k given in the parenthesis. The rest of the response variables are modelled with Gaussian distribution and identity link (Model 1). Edf stands for estimated degrees of freedom. VarPower refers to power of covariate variance structure, with the estimated exponent given in the parenthesis.

		Intercept		Day		*Day* JellyC*				
Response variable	Units	Estimate	*P*	edf	*P*	edf	*P*	R^2 (adj)	*n*	Adjustments
Bacteria (HNA)	cells mL^{-1}	1 527 153	***	6.2	***	–	ns	0.67	88	
Bacteria (LNA)	cells mL^{-1}	594 329	***	5.7	***	–	ns	0.36	88	
Bacterial production	μg C L^{-1} h^{-1}	0.178	***	–	ns	5.4	***	0.53	87[a]	
Bacterial production	μg C L^{-1} h^{-1}	0.178	***	6.0	***	2.6	***	0.58	86[a,b]	
BP per cell	pg C $cell^{-1}$ h^{-1}	0.088	***	5.7	***	3.4	***	0.60	87[a]	
Chl *a* <10 μm	μg L^{-1}	1.84	***	5.7	***	–	ns	0.71	88	
Chl *a* >10 μm	μg L^{-1}	0.46	***	6.7	***	7.3	***	0.97	88	varPower (0.91)
Ciliates	cells L^{-1}	10.05	***	3.7	***	2.9	0.04	0.89	55[c]	NB (17.8)
Cryptophytes	cells mL^{-1}	7.01	***	6.5	***	–	ns	0.71	87[d]	NB (15.8)
DOC	mg L^{-1}	1.71	***	–	ns	–	ns	−0.04[e]	77[f]	
E. huxleyi	cells mL^{-1}	3.4	***	6.8	***	–	ns	0.86	87[d]	NB (11.6)
HNF	cells mL^{-1}	8.47	***	4.0	***	–	ns	0.85	45[g]	NB (25.6)
Nanoplankton	cells mL^{-1}	8.2	***	6.7	***	–	ns	0.83	87[d]	NB (22)
NH_4	μmol L^{-1}	4.42	***	6.6	***	2	***	0.92	88	
Nitrate	μmol L^{-1}	9.92	***	5.4	***	–	ns	0.40	88	
Nitrite	μmol L^{-1}	0.19	***	–	ns	2	***	0.58	88	
Phosphate	μmol L^{-1}	0.97	***	6.7	***	2	***	0.60	88	
Picoplankton	cells mL^{-1}	9.97	***	6.6	***	2.2	0.02	0.84	87[d]	NB (7.4)
POC	mg L^{-1}	0.24	***	5.9	***	–	ns	0.71	86[h,i]	varPower(0.51)
PON	mg L^{-1}	0.043	***	5.8	***	–	ns	0.76	87[h]	varPower(0.64)
Primary production	μg C L^{-1} h^{-1}	31.49	***	6.6	***	3.3	***	0.85	88	varPower(0.67)
Prim. prod. per Chl *a*	μg C μg Chl a^{-1} h^{-1}	16.98	***	6.0	***	2	0.005	0.40	88	varPower(−0.95)
Silicate	μmol L^{-1}	4.48	***	6.7	***	–	ns	0.93	88	
Synechococcus	cells mL^{-1}	11.12	***	6.2	***	2	0.01	0.83	87[d]	NB (43.6)
TOC	mg L^{-1}	1.87	***	1	0.05	–	ns	0.11	77[f]	
Virus	Virus mL^{-1}	20 424 477	***	6.5	***	–	ns	0.52	88	

[a]Negative outlier removed (D7M3).
[b]Removal of additional influential high outlier (D8M6) changes results and considerably improves the behaviour of residuals.
[c]Days 1, 2, 4, 6 and 8.
[d]D5M9 is removed from all flow cytometer autotroph measurements due to unrealistically low values.
[e]$R^2 < 0$ implies that the model is worse than a one-parameter constant model.
[f]Missing Day 1.
[g]Days 2, 5, 7, 8 and two samples (M1 and M3) from Day 1;missing D5M12.
[h]Missing one observation.
[i]Outlier removed (D1M5).
D and M in the footnotes refer to sample day and mesocosm, respectively. Only estimates with *P*-values <0.05 are shown; ***for $P < 0.001$, ns for not significant; note that *P*-values in GAMM should be interpreted conservatively (Zuur *et al.*, 2009).

(Table II). Gaussian distribution with identity link was used for continuous response variables as well as the very high bacterial and viral abundances (Model 1, Table II). Due to observed over-dispersion, negative binomial distribution with log link was used for other counts (Model 2, Table II), with the dispersion parameter k adjusted manually to the accuracy of one decimal place by finding scale estimate approaching 1. The applied models allow for a non-linear development with time (*Day*) and assume a linear response to *JellyC* (but note log link in Model 2). Since the response to *JellyC* develops over time from a common starting point (i.e. no effect) for all *JellyC* concentrations, an interaction between *Day* and *JellyC* is included in the model, allowing the response to develop in time. Tensor product interaction was used due to the different scales of these explanatory variables. Since the rate of internal circulation varied between mesocosms, a linear explanatory variable *Flow* was initially included in the models. However, as *Flow* was not significant for any of the explanatory variables studied ($P > 0.05$), it was excluded from the final models. The fitted models were thus specified as follows:

$$\text{Model 1 } \mathrm{RV}_i = \alpha + f_1(\mathrm{Day}_i) + f_2(\mathrm{Day}_i : \beta_1 \mathrm{JellyC}_i) + \varepsilon_i$$

$$\varepsilon_i \sim N(0, \sigma^2)$$

$$\text{Model 2 } \mathrm{RV}_i \sim \mathrm{NB}(\mu_i, k); E(\mathrm{RV}_i) = \mu_i; \mathrm{Var}(\mathrm{RV}_i) = \frac{\mu_i + \mu_i^2}{k}$$

$$\log(\mu_i) = \alpha + f_1(Day_i) + f_2(\mathrm{Day}_i : \beta_1 \mathrm{JellyC}_i)$$

where RV is the response variable to be modelled. Model 2 was applied both to raw counts with log of sample volume as offset, and to concentrations (cells mL^{-1}) rounded to closest integer. As the minor loss of accuracy in the latter method did not change the resulting conclusions, this method was applied for easier interpretation of results. A first order autoregressive correlation (AR-1) was included in all models to account for temporal autocorrelation between sequential observations within each mesocosm.

A few obviously incorrect values (e.g. negative measurements) were removed during data exploration (see Table II for details). Mesocosm 2 contained a dead jellyfish at the end and was excluded from analyses to prevent effects by the decomposing carcass. Model adequacy was assessed by examining scatter plots of observed values versus fitted values and residuals from the models, as well as overdispersion plots (Olive, 2013) for Model 2. For Model 1, a power variance structure was applied if residual heterogeneity was observed to allow for altered variance with time (Table II). Log likelihood tests used to compare the models with and without power variance structure showed that the former model was the better choice in all of these cases ($P < 0.0001$).

Data exploration and analyses were conducted with R version 2.15.3 (R Core Team, 2013). Figures were plotted with R version 2.15.3 and Sigmaplot 11.0.

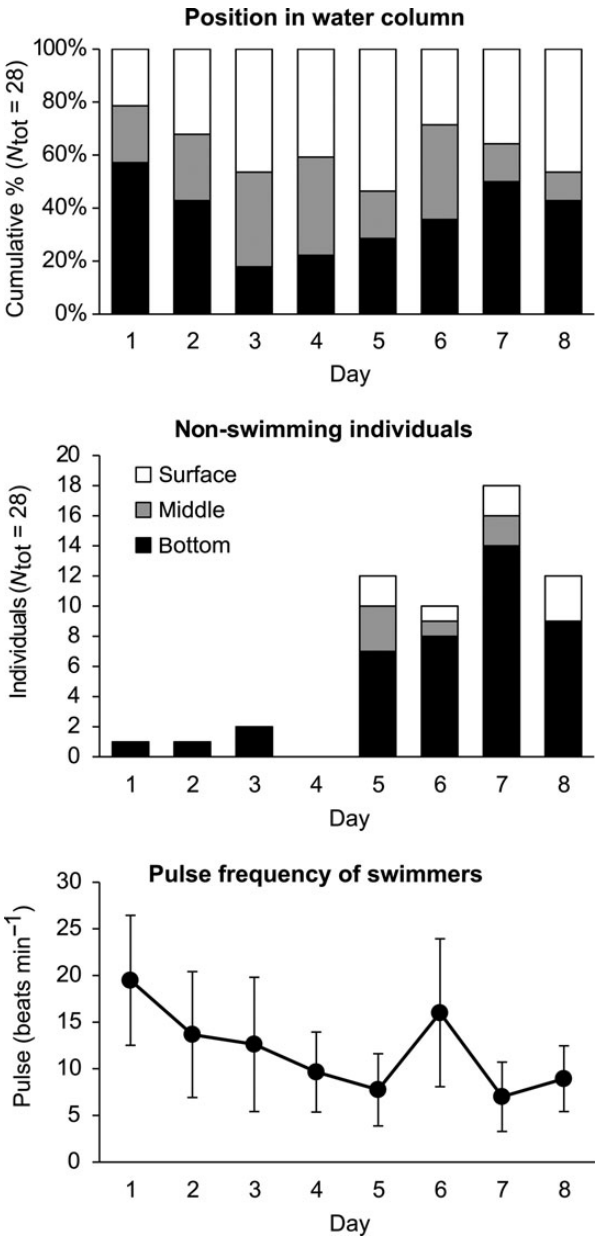

Fig. 2. Jellyfish condition during the experiment. Upper panel shows the vertical distribution of all jellyfish in the mesocosms (see middle panel for legend). Middle panel shows the number or inactive individuals at the time of the daily monitoring and their vertical distribution in the mesocosms. The lower panel shows the pulse frequency (mean and SD) of the active individuals.

RESULTS

Jellyfish condition

All jellyfish appeared healthy and active at the start of the experiment. Vertical distribution of the jellyfish in the mesocosms remained similar throughout the experiment (Fig. 2). However, there was a considerable increase in the proportion of jellyfish not actively swimming after Day 4, particularly among those located close to the bottom of the mesocosms, and the average pulse frequency of active individuals also decreased during the experiment (Fig. 2). These jellyfish should nevertheless not be considered dead, as in many cases those that were inactive at the time of the vitality monitoring were observed swimming some time later. Also, all but one jellyfish in mesocosm 2 responded to stimuli by pulsing at the end of the experiment. The diameter of the jellyfish at the end of the experiment was 10.9 ± 2.4 cm (mean and SD). At the end of the experiments, 11 of the 28 jellyfish carried planula larvae, 12 showed some damage to lappets or bell, and a few had clearly lost some feeding structures.

Seawater chemistry, carbon and nutrients

Temperature, salinity and oxygen concentration varied little between mesocosms, although conditions overall changed slightly during the experiment, partly due to weather conditions (Table III).

Ammonium, nitrite and phosphate concentrations responded to *JellyC*, indicating nutrient recycling by the jellyfish (Fig. 3, Table II). Phosphate levels remained

Table III: Seawater chemistry during the experiment, mean ± SD for all mesocosms

	Start (Day 1)	End (Day 8)
T (°C)	13.95 ± 0.14	10.43 ± 0.32
Salinity	29.90 ± 0.00	28.53 ± 0.50
O_2 (mg L^{-1})	8.47 ± 0.05	8.26 ± 0.05

relatively stable over time apart from a peculiar peak on Day 2. Changes in the dissolved inorganic nitrogen pool were dominated by ammonium, which exhibited the largest variation with respect to both time and treatment. Silicate levels decreased at an increasing rate, without discernible effect of *JellyC* (Fig. 4F). The N/P ratio in the mesocosms fluctuated around the Redfield ratio (Fig. 4G).

As the experiment progressed, POC and PON levels increased in a similar manner (Fig. 4A and B). TOC subsequently showed a similar increase, while DOC levels remained at the same level, despite fluctuation in TOC measurements (Fig. 4C and D).

Community succession

The pelagic community in all mesocosms followed a similar succession in time, on which the effects of *JellyC* were superimposed. Following the nutrient addition at the beginning of the experiment, all mesocosms experienced a rapid increase in autotrophic picoplankton during Days 1–4 (Fig. 4I and J). After Day 4, picoplankton abundances stopped increasing and started declining, probably due to increased predation by HNFs (Fig. 4M). Reduced competition from picoplankton allowed the larger autotrophic nanoplankton and, more slowly, diatoms (with the >10 μm chl *a* as a proxy) to increase in abundance (Fig. 3, Fig. 4K and L). The HNF populations in turn crashed on Day 8, probably due to predation by the exponentially increasing ciliates (Fig. 4M and N).

Mesozooplankton

There were no significant differences between the abundances of the main mesozooplankton groups in the start samples or between treatments in the end (MANOVA, $P = 0.18$; Fig. 5). Mesozooplankton community composition showed a borderline significant difference between start and end (*adonis*, $F = 2.88$, $R^2 = 0.16$, $P = 0.056$), but no effect of treatment or *JellyC*. Temporal autocorrelation was not considered in the analyses, since start samples were taken in between filling of the mesocosms. The most numerous copepods were *Oithona* sp. and other cyclopoids, *Para-/Pseudocalanus* sp. and, in the end samples, *Clytemnestra* sp. Appendicularians *Oikopleura* sp. and, to a lesser degree, *Fritillaria* sp. were moderately abundant at the start, but virtually absent at the end. Polychaete and gastropod larvae dominated the meroplankton. The most notable change in mesozooplankton during the experiment was a reduction in meroplankton abundance across all treatments (Fig. 5).

Phytoplankton community composition and chlorophyll *a*

Phytoplankton community composition showed a temporal succession with significant differences between Days 1, 4 and 8 (*adonis*, $F = 11.98$, $R^2 = 0.43$, $P = 0.0001$). No significant differences between treatments or interactions between treatment and time were observed. The community included a large number of mixotrophs. On Days 1 and 4, phytoplankton counts were dominated by dinoflagellates, especially *Protoperidium* sp., *Scripsiella*-group, *Prorocentrum* spp., *Gyrodinium* spp., *Gymnodinium* sp., *Dinophysis* spp. and *Ceratium* spp. By Day 8, the composition changed noticeably: while many dinoflagellates were still abundant, the numeric dominance shifted to diatoms (*Pseudo-nitzschia* sp., *Eucampia* sp., *Skeletonema* sp., *Thalassiosira* sp. and other centric diatoms). Choanoflagellates increased in abundance from Day 4 to Day 8 in all mesocosms, while the euglenophyte *Eutreptiella* sp. became more numerous in some. In addition, cryptophytes and silicoflagellate *Dictyocha speculum* were present throughout the experiment. The main autotrophic groups in the flow cytometer counts were *Synechococcus*, unidentfied picoeukaryotes, nanoplankton (two size groups, combined in the analyses), cryptophytes and relatively low numbers of *E. huxleyi* (Fig. 3I–L).

Concentration of the <10 μm chl *a* size fraction during the experiment mirrored the combined abundances of autotrophic pico- and nanoplankton, with no apparent effect of *JellyC* (Fig. 4H). The exponential increase in the concentration of the >10 μm chl *a* size fraction towards the end of the experiment (Fig. 3) and the decrease in silicate concentrations (Fig. 4F) reflected the concurrent shift to diatom dominance.

Bacterial community composition

A total of 136 420 partial 16S rRNA gene sequences remained after quality controls, yielding on average 4870 reads per samples (range 2618–8585 reads) and a total of 809 unique OTUs in the entire dataset. The community compositions over time in the different treatments were compared using PCA of the weighted-UniFrac distances between normalized samples. The change in community composition with time was similar in all treatments, and no major differences were observed.

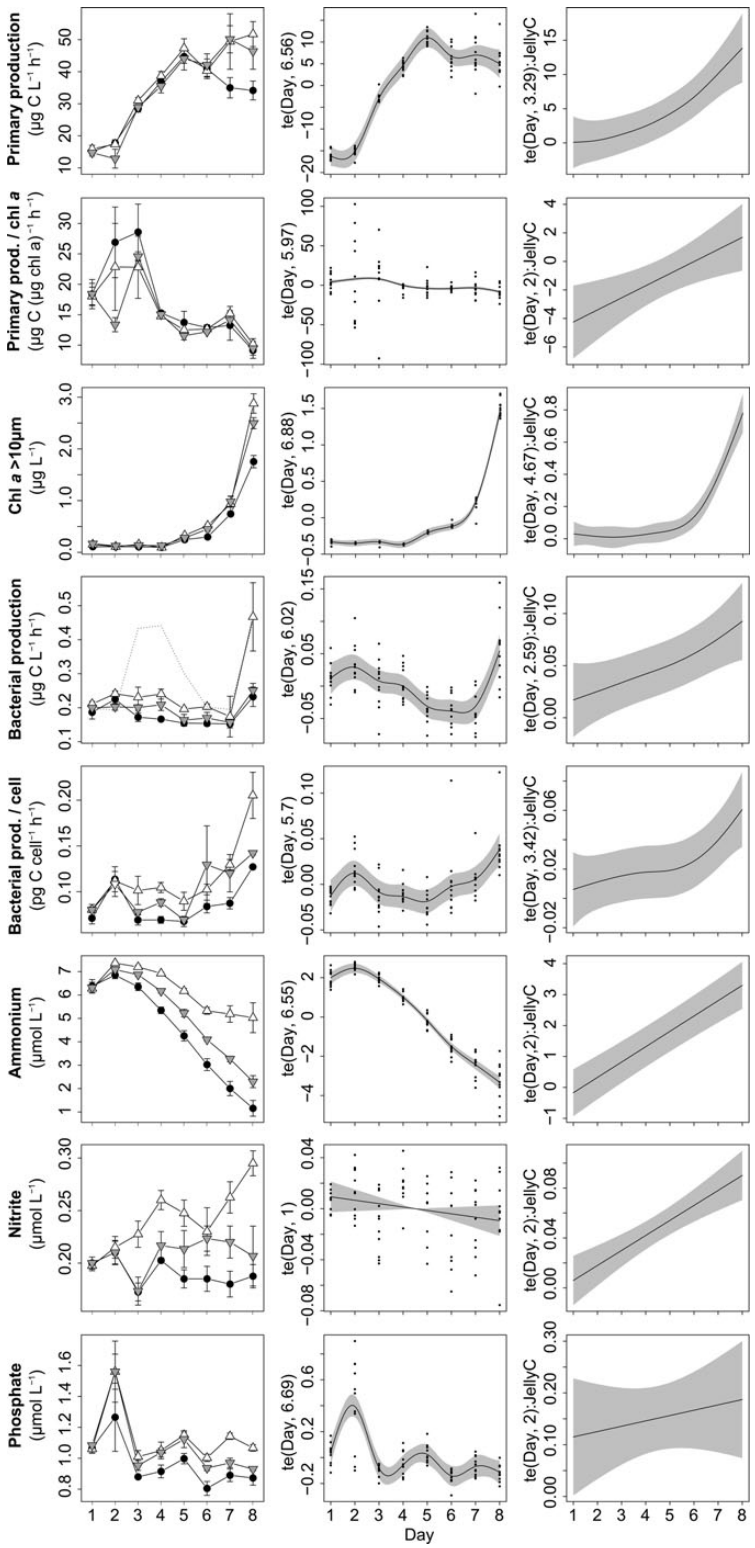

Fig. 3. Response variables with a highly significant ($P \leq 0.005$) *Day*JellyC* interaction in GAMM. Left panels show the original data (mean ± SE) grouped by treatment. Controls, 2 *Cyanea* and 5 *Cyanea* treatments are indicated by black dots, grey downward triangles and white upward triangles, respectively. Dotted line in bacterial production (row 4) shows values for mesocosm 2, excluded from analyses due to a dead jellyfish. Second panels show the GAMM smooth for *Day*, with 95% CI (2 × SE) and partial residuals. Right panels show the GAMM smooth and 95% CI for the *Day*JellyC* interaction in terms of additive adjustment of response variable per 1 mg *JellyC* L^{-1}. See Table II for detailed model results.

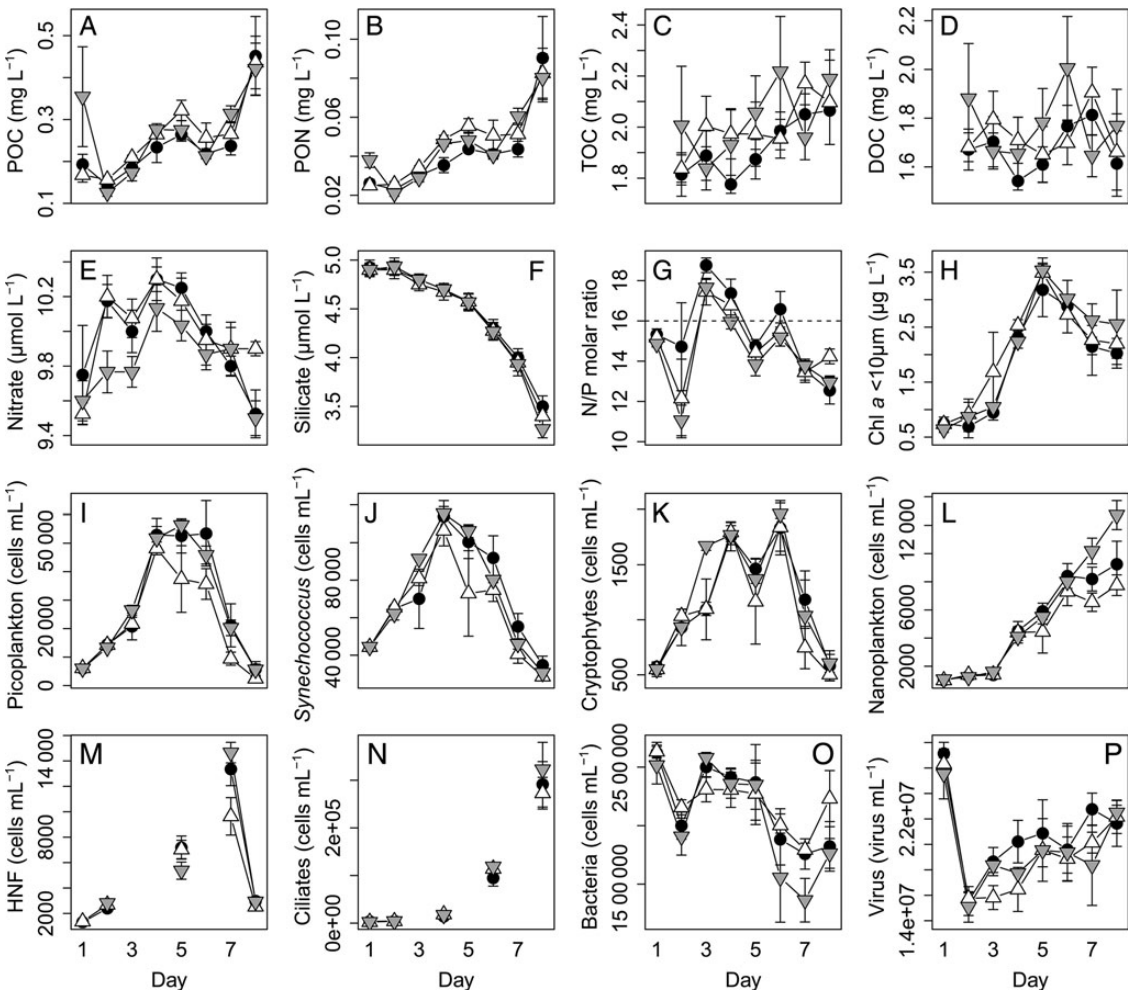

Fig. 4. Response variables for which no highly significant *Day*JellyC* interaction was observed, mean + SE. Controls, 2 *Cyanea* and 5 *Cyanea* treatments are indicated by black dots, grey downward triangles and white upward triangles, respectively. Horizontal line in panel G indicates the Redfield ratio; Panel L shows abundance of nanoplankton including *E. huxleyi*; Panel O shows combined abundance of LNA and HNA bacteria.

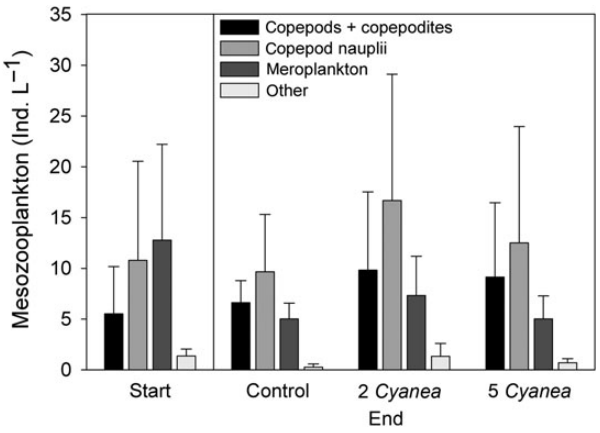

Fig. 5. Abundances of main groups of mesozooplankton at the start and in different treatments at the end of the experiment, mean ± SD.

Primary and bacterial production

Primary production per unit biomass (µg C µg chl a^{-1} h^{-1}) was similar in all treatments, apart from Days 2–3, when variation was large and the controls showed highest average values (Fig. 3). The significant *day*JellyC* interaction, with a negative influence of *JellyC* in the start, is likely much influenced by these 2 days. The total primary production per volume (µg C L^{-1} h^{-1}) reflected the total concentration of chl *a*, with an increased influence of *JellyC* towards the end of the experiment when diatoms began to dominate (Fig. 3).

JellyC elevated both total and cell-specific bacterial production throughout the experiment, with somewhat increased effect towards the end (Fig. 3).

Results from GAMM

All modelled response variables apart from nitrite, DOC and TOC changed significantly over time, with similar main patterns across treatments (Table II, Figs 3 and 4). This general pattern was for some response variables further modified by the presence of jellyfish, as indicated by the highly significant *Day*JellyC* interaction for several nutrients, >10 μm chl *a* fraction, total primary production and bacterial production. For bacterial production, removing a single influential high outlier significantly changed the results and improved the behaviour of outliers (Table II); however, the *Day*JellyC* interaction was highly significant both with and without the outlier. The recommendation to interpret *P*-values from GAMM conservatively (Zuur *et al.*, 2009) should be taken into account when considering the results with a *P*-value closer to 0.05.

DISCUSSION

Although *C. capillata* is known to feed readily in captivity (e.g. Båmstedt *et al.*, 1994; Hosia and Titelman, 2011), and has been successfully used for predation experiments also in the very same tanks that we used (Titelman *et al.*, 2007), the jellyfish in our experiment had no noticeable effect on the abundance or community composition of mesozooplankton. Similarly, no cascading top-down effects were observed for large phytoplankton or ciliates. This is surprising, as applying even a conservative clearance rate of 5 L h^{-1} ind^{-1} (cf. Fancett and Jenkins, 1988; Båmstedt *et al.*, 1994; Sørnes and Aksnes, 2004) with 100% capture efficiency would result in expected daily zooplankton losses of ~10 and ~24% in the 2 and 5 *Cyanea* treatments, respectively.

This unexpected lack of predatory impact is probably related to the observed deterioration of jellyfish vitality during the experiment (Fig. 1). The jellyfish were collected with care, appeared healthy at the start of the experiment and were not handled during the experiment, but we cannot rule out that they were nevertheless stressed by the experimental conditions, for example the decrease in the temperature. The lack of predatory impact could also be due to the timing of the experiment, relatively late in the season for *C. capillata* jellyfish. In southern Norway, *C. capillata* typically reaches maximum abundances in June, with the season's last individuals observed in November–December (Hosia *et al.*, 2014). It has been suggested that the appearance of blastulae on the oral arms of *Cyanea* towards the end of their annual season occurs simultaneously with the degeneration of feeding structures and is followed by deterioration and death (Brewer, 1989). Even in the early stages of this decaying process, the jellyfish are unable to feed (Brewer, 1989). It could thus be that the jellyfish in our experiment, many of which were carrying planulae at the end of the experiment, were becoming senescent and had reduced feeding.

Apart from the jellyfish biomass, the start conditions in the mesocosms were identical. Since no top-down impacts from jellyfish predation were evident, we can assume that the observed differences developed due to bottom-up mediated effects from the jellyfish.

The concentration of *JellyC* translated to increasing differences in N and P concentrations during the experiment (Table II, Fig. 3). No clear effect of jellyfish on primary production per unit biomass was observed. Nevertheless, jellyfish boosted the larger chl *a* fraction, primarily diatoms and correspondingly total primary production towards the end of the experiment (Table II, Fig. 3). The observed mesozooplankton abundances and top-down pathways fail to explain these effects. It is possible that small, undetected differences in normalized primary production resulted in noticeable effects due to the exponential growth of the diatoms at this stage. This exponential growth was facilitated by the increased availability of nutrients combined with decreased competition from picoplankton and bacteria declining in abundance. While small autotrophs initially responded fastest to the nutrient additions, their population growth was curbed by predation by HNFs. Autotrophs in general seemed to benefit from the diminished nutrient limitation more than bacteria, suggesting that availability of labile DOC may have been limiting bacterial production. Primary production, on the other hand, was light limited during our experiment, as indicated by much higher rates (73.7 ± 7.4 μg C L^{-1} h^{-1}, mean ± SD for all mesocosms, measured on Day 5) achieved when replicate samples were incubated in algal culture rooms with comparable temperatures but higher light intensities.

Under oligotrophic conditions, abundant jellyfish can be a significant source of nutrients for primary producers (reviewed in Pitt *et al.*, 2009). *In situ*, nitrogen was limiting production in the surface waters at the time of our experiment (concentrations measured 26 September 2011 from ~10 m depth: $NO_2 < 0.06$, $NO_3 < 0.4$ and PO_4 1.79 μmol L^{-1}). Under such conditions, the excretion of nitrogenous compounds by abundant jellyfish could have a noticeable impact on productivity. We added inorganic nutrients to all mesocosms prior to experiment start to avoid potential nutrient limitation of primary and secondary producers masking the effects caused by the jellyfish (cf. Dinasquet *et al.*, 2012a). In hindsight, it would have been interesting to also have included treatments without added nutrients; effects of nutrient regeneration by jellyfish could have been more pronounced in the nutrient depleted waters, and both lower nutrient levels and

the lack of silicate in such a scenario could have favoured the smaller autotrophs.

The presence of jellyfish consistently stimulated bacterial production. This was probably due to release of colloidal and dissolved organic matter by the jellyfish (Hansson and Norrman, 1995; Condon *et al.*, 2011). Jellyfish produce copious amounts of mucus, in addition to other excretions, leakage of DOC, sloppy feeding and egestion of undigested prey (Pitt *et al.*, 2009). The organic carbon released was either rapidly taken up by the bacteria, or below the detection level of our DOC measurements. While we are not aware of any estimates on DOC excretion by *Cyanea* spp., the average release of DOC by *Aurelia aurita* medusae of 9.5–18 cm diameter from the Skagerrak has been estimated as 1.2 mg C ind.$^{-1}$ day^{-1} (Hansson and Norrman, 1995). Applying this number would give an increase of ~2.4 mg C day^{-1} for the 2 *Cyanea* treatments and ~6 mg C day^{-1} for the 5 *Cyanea* treatments, i.e. 0.001 mg C L^{-1} day^{-1} and 0.0024 mg C L^{-1} day^{-1}. Considering the precision of our measurements, this would not be a noticeable addition to the observed background DOC levels (~1.7 mg C L^{-1}). However, bulk of the measured background DOC may not have been readily available for bacteria, while the dissolved organic matter released by the jellyfish is extremely labile and rapidly utilized by bacteria (Condon *et al.*, 2011, Dinasquet *et al.*, 2013).

While jellyfish stimulated both total and specific bacterial production, bacterial abundance was unaffected by jellyfish. This may have been partly due to predation by viruses, HNF and mixotrophic protists. For unknown reasons, there were differences in HNF abundances between the treatments during the HNF peak on Day 7 (ANOVA, $F_{(2,8)} = 5.845$, $P = 0.027$), with the low *JellyC* treatment having the highest concentration of HNF and the high *JellyC* treatment the lowest (Fig. 4M). Bacterial abundances seemed to mirror this pattern, hinting towards grazing control. This is further supported by increased bacterial production and increased proportion of HNA versus LNA bacterial cells (data not shown) accompanying the drop in HNF abundance towards the end of the experiment.

Bacterial community composition and succession were not affected by the jellyfish. In contrast, other studies have observed changes in bacterial community in response to DOM from live jellyfish (Condon *et al.*, 2011; Dinasquet *et al.*, 2012b; Hao, 2014), decomposing jellyfish (Titelman *et al.*, 2006; Frost *et al.*, 2012) or homogenized jellyfish (Tinta *et al.*, 2010; Tinta *et al.*, 2012). On the other hand, in another Nordic mesocosm experiment, the ctenophore *Mnemiopsis leidyi* also failed to induce discernible changes in bacterial community composition (Dinasquet *et al.*, 2012a). Possibly the effects of jellyfish on the bacterial community are most noticeable in close proximity to the jellyfish and become diluted in the larger mesocosms or *in situ* (Hansson and Norrman, 1995; Dinasquet *et al.*, 2012b, 2013), unless jellyfish concentrations are enormous or persistent over time (cf. Lurefjorden, Riemann *et al.*, 2006).

Potentially, the senescent state of our jellyfish resulted in higher than normal leakage of organic carbon and nutrients, and differences in their decomposition stage may have contributed to variation between mesocosms (cf. Frost *et al.*, 2012). Similarly, jellyfish in different stages of senescence may have caused random variation in the predatory impact on mesozooplankton across the treatments, resulting in the relatively large within treatment variation in the end mesozooplankton abundances (Fig. 4). While moribund, all of our jellyfish apart from one were nevertheless still alive and responding to stimuli at the end of the experiment. Interestingly, the mesocosm with the dead jellyfish had the highest bacterial production during Days 2–4 (Fig. 3). A number of parasitic hyperiid amphipods were found associated with the jellyfish at the end of the experiment, and could also have contributed to the observed bottom-up effects. These amphipods may also play a role in the demise of scyphozoan populations in the autumn (Lauckner, 1980).

While the *C. capillata* in our experiment clearly stimulated phytoplankton and bacterial production, the relative importance of the bottom-up impact of jellyfish is likely to vary. Jellyfish species differ in their seasonal occurrence, and whether their bottom-up influence is of consequence will partly depend on concurrent nutrient conditions, pelagic community composition and biological interactions. Clearly, impacts are likely to be most conspicuous when dense blooms occur in oligotrophic waters. Excretion of both organic carbon and inorganic nutrients by jellyfish appears to increase with temperature (reviewed by Pitt *et al.*, 2009), suggesting stronger effects in warmer regions or seasons. Jellyfish species also differ in terms of their DOM excretion and nutrient regeneration rates. For example, the ctenophore *Mnemiopsis leidyi* excretes more ammonium and releases DOM richer in carbon than does the scyphozoan *Chrysaora quinquecirrha* (Condon *et al.*, 2011). There are some indications that bacterial responses vary depending on jellyfish species (Titelman *et al.*, 2006; Condon *et al.*, 2011; Hao, 2014). The simultaneous predatory top-down effect also varies between species, which may feed selectively and at different rates (Purcell, 1997).

Despite such variation, it is clear that the impact of jellyfish in the pelagic system is not limited to their role as predators, but also includes bottom-up influences on the productivity and structure of lower trophic levels, as well as their contribution to the vertical flux of carbon. These effects will be particularly pronounced in connection with

jellyfish blooms and, as is demonstrated by our study, the relative importance of top-down and bottom-up effects may change through the different stages of a bloom as the jellyfish complete their lifecycle. So far, these important aspects of jellyfish ecology have received relatively little attention.

ACKNOWLEDGEMENTS

We thank the following people: Agnes Aadnes and Tomas Sørlie at Espegrend Marine Biological station for facilities, technical assistance and help in jellyfishing. Jorun K. Egge for help in planning the experiment, comments on the manuscript and equipment loan; Tron Frede Thingstad, Jean-Marie Bouquet and Eric Thompson for equipment loan; Jessica Rey for virus data and help with the FCM; Tom Andersen for discussions regarding statistics; Anne Jähkel for practical help; Knut Yngve Børsheim and Are Olsen for help with TOC and DIC, respectively; Marianne Pettersen and Linda Fonnes Lunde for the chemical analyses; Monica Martinussen for zooplankton counts and practical help; Eli Gustad and Mona Ring Kleiven for phytoplankton counts.

DATA ARCHIVING

All sequences obtained in this study have been deposited in the European Nucleotide Archive—Short Read Archive under the accession number PRJEB7907.

FUNDING

This work was supported by the Research Council of Norway (190304/S40 to A.H., C.B.A. and O.S.; 210460 to A.H.); the Norwegian Biodiversity Information Centre (Artsdatabanken) (70184215 to A.H.); the BONUS+ project BAZOOCA (Baltic Zooplankton Cascades) (210-2008-1882 to L.G.; FORMAS 2008-1893 through the Swedish Research Council for Environment Agricultural Sciences and Spatial Planning to L.R.) and Walter and Andrée de Nottbeck Foundation and University of Helsinki (to J.M.R.).

REFERENCES

Båmstedt, U., Martinussen, M. B. and Matsakis, S. (1994) Trophodynamics of the two scyphozoan jellyfishes, *Aurelia aurita* and *Cyanea capillata*, in western Norway. *ICES J. Mar. Sci.*, **51**, 369–382.

Boström, K. H., Simu, K., Hagström, Å. and Riemann, L. (2004) Optimization of DNA extraction for quantitative marine bacterioplankton community analysis. *Limnol. Oceanogr. Methods*, **2**, 365–373.

Bratbak, G. and Dundas, I. (1984) Bacterial dry matter content and biomass estimations. *Appl. Environ. Microbiol.*, **10**, 755–757.

Bratbak, G., Jacquet, S., Larsen, A., Pettersson, L. H., Sazhin, A. F. and Thyrhaug, R. (2011) The plankton community in Norwegian coastal waters—abundance, composition, spatial distribution and diel variation. *Cont. Shelf Res.*, **31**, 1500–1514.

Brewer, R. H. (1989) The annual pattern of feeding, growth and sexual reproduction in *Cyanea* (Cnidaria: Scyphozoa) in the Niantic River estuary, Connecticut. *Biol. Bull.*, **176**, 272–281.

Caporaso, J. G., Kuczynski, J., Stombaugh, J., Bittinger, K., Bushman, F. D., Costello, E. K., Fierer, N., Pena, A. G. *et al.* (2010) QIIME allows analysis of high-throughput community sequencing data. *Nat. Methods*, **7**, 335–336.

Condon, R. H., Steinberg, D. K., Del Giorgio, P. A., Bouvier, T. C., Bronk, D. A., Graham, W. M. and Ducklow, H. W. (2011) Jellyfish blooms result in a major microbial respiratory sink of carbon in marine systems. *PNAS*, **108**, 10225–10230.

Dickson, A. G., Sabine, C. L. and Christian, J. R. (2007) *Guide to Best Practices for Ocean CO2 Measurements*. North Pacific Marine Science Organization, Sidney, British Columbia (PICES Special Publication, 3).

Dinasquet, J., Granhag, L. M. and Riemann, L. (2012b) Stimulated bacterioplankton growth and selection for certain bacterial taxa in the vicinity of the ctenophore *Mnemiopsis leidyi*. *Front. Microbiol.*, **3**, article 302, 1–8.

Dinasquet, J., Kragh, T., Schrøter, M.-L., Søndergaard, M. and Riemann, L. (2013) Functional and compositional succession of bacterioplankton in response to a gradient in bioavailable dissolved organic carbon. *Environ. Microbiol.*, **15**, 2616–2628.

Dinasquet, J., Titelman, J., Møller, L. F., Setälä, O., Granhag, L., Andersen, T., Båmstedt, U., Haraldsson, M. *et al.* (2012a) Cascading effects of the ctenophore *Mnemiopsis leidyi* on the planktonic food web in a nutrient-limited estuarine system. *Mar. Ecol. Prog. Ser.*, **460**, 49–61.

Fancett, M. S. and Jenkins, G. P. (1988) Predatory impact of scyphomedusae on ichthyoplankton and other zooplankton in Port Phillip Bay. *J. Exp. Mar. Biol. Ecol.*, **116**, 63–77.

Frost, J. R., Jacoby, C. A., Frazer, T. K. and Zimmerman, A. R. (2012) Pulse perturbations from bacterial decomposition of *Chrysaora quinquecirrha* (Scyphozoa: Pelagiidae). *Hydrobiologia*, **690**, 247–256.

Granéli, E. and Turner, J. T. (2002) Top-down regulation in ctenophore-copepod-ciliate-diatom-phytoflagellate communities in coastal waters: a mesocosm study. *Mar. Ecol. Prog. Ser.*, **239**, 57–68.

Grasshof, K., Ehrhart, M. and Kremling, F. (1983) *Methods of Seawater Analysis*. 2nd edn. Verlag Chemie, Wiley, Weinheim, pp. 410.

Hansson, L. J. and Norrman, B. (1995) Release of dissolved organic carbon (DOC) by the scyphozoan jellyfish *Aurelia aurita* and its potential influence on the production of planktic bacteria. *Mar. Biol.*, **121**, 527–532.

Hao, W. (2014) Bacterial community associated with jellyfish. PhD Thesis. University of Bremen.

Hosia, A., Falkenhaug, T. and Naustvoll, L. J. (2014) Trends in abundance and phenology of *Aurelia aurita* and *Cyanea* spp. at a Skagerrak location, 1992–2011. *Mar. Ecol. Prog. Ser.*, **498**, 103–115.

Hosia, A. and Titelman, J. (2011) Intraguild predation between the native North Sea jellyfish *Cyanea capillata* and the invasive ctenophore *Mnemiopsis leidyi*. *J. Plankton Res.*, **33**, 535–540.

Huete-Stauffer, T. and Morán, X. (2012) Dynamics of heterotrophic bacteria in temperate coastal waters: similar net growth but different

controls in low and high nucleic acid cells. *Aquat. Microb. Ecol.*, **67**, 211–223.

Johnson, K. M., King, A. E. and Sieburth, J. M. (1985) Coulometric TCO_2 analyses for marine studies; an introduction. *Mar. Chem.*, **16**, 61–82.

Kuuppo-Leinikki, P. and Kuosa, H. (1989) Preservation of picoplanktonic cyanobacteria and heterotrophic nanoflagellates for epifluorescence microscopy. *Arch. Hydrobiol.*, **114**, 631–636.

Lauckner, G. (1980) Diseases of Cnidaria. In: Kinne, O. (ed.) *Diseases of Marine Animals*, Vol. I. Wiley, New York, pp. 167–238.

Lebrato, M., De Jesus Mendes, P., Steinberg, D. K., Cartes, J. E., Jones, B. M., Birsa, L. M. and Benavides, R. (2013) Jelly biomass sinking speed reveals a fast carbon export mechanism. *Limnol. Oceanogr.*, **58**, 1113–1122.

Lucas, C. H., Jones, D. O. B., Hollyhead, C. J., Condon, R. H., Duarte, C. M., Graham, W. M., Robinson, K. L., Pitt, K. A. *et al.* (2014) Gelatinous zooplankton biomass in the global oceans: geographic variation and environmental drivers. *Global Ecol. Biogeogr.*, **23**, 701–714.

Marie, D., Brussaard, C. P. D., Thyrhaug, R., Bratbak, G. and Vaulot, D. (1999) Enumeration of marine viruses in culture and natural samples by flow cytometry. *Appl. Environ. Microb.*, **65**, 45–52.

Martinussen, M. B. and Båmstedt, U. (1995) Diet, estimated daily food ration and predator impact by the scyphozoan jellyfishes *Aurelia aurita* and *Cyanea capillata*. In Skjoldal, H. R., Hopkins, C., Erikstad, K. E. and Leinaas, H. P. (eds), *Ecology of Fjords and Coastal Waters*. Elsevier Science B.V., pp. 127–145.

McNamara, M. E., Lonsdale, D. J. and Cerrato, R. M. (2014) Role of eutrophication in structuring planktonic communities in the presence of the ctenophore *Mnemiopsis leidyi*. *Mar. Ecol. Prog. Ser.*, **510**, 151–165.

Niemi, M., Kuparinen, J., Uusi-Rauva, A. and Korhonen, K. (1983) Preparation of ^{14}C-labeled algal samples for liquid scintillation counting. *Hydrobiologia*, **106**, 149–156.

Oksanen, J., Blanchet, F. G., Kindt, R., Legendre, P., Minchin, P. R., O'Hara, R. B, Simpson, L. G., Solymos, P. *et al.* (2013). *vegan: Community Ecology Package*. R package version 2.0–9. http://CRAN.R-project.org/package=vegan.

Olive, D. J. (2013) Plots for generalized additive models. *Comm. Statist. Theory Methods*, **42**, 3310–3328.

Pitt, K. A., Welsh, D. T. and Condon, R. H. (2009) Influence of jellyfish blooms on carbon, nitrogen and phosphorus cycling and plankton production. *Hydrobiologia*, **616**, 133–149.

Purcell, J. E. (1997) Pelagic cnidarians and ctenophores as predators: selective predation, feeding rates, and effects on prey populations. *Ann. Inst. Oceanogr.*, **73**, 125–137.

Purcell, J. E., Uye, S. and Lo, W. T. (2007) Anthropogenic causes of jellyfish blooms and their direct consequences for humans: a review. *Mar. Ecol. Prog. Ser.*, **350**, 153–174.

R Core Team. (2013). R: A language and environment for statistical computing. R Foundation for Statistical Computing, Vienna, Austria. ISBN 3-900051-07-0, URL http://www.R-project.org/.

Riemann, B., Bjørnsen, P. K., Newell, S. and Fallon, R. (1987) Calculation of cell production of coastal marine bacteria based on measured incorporation of [^{3}H]thymidine. *Limnol. Oceanogr.*, **32**, 471–476.

Riemann, L., Steward, G. F. and Azam, F. (2000) Dynamics of bacterial community composition and activity during a mesocosm diatom bloom. *App. Env. Microbiol.*, **66**, 578–587.

Riemann, L., Titelman, J. and Båmstedt, U. (2006) Links between jellyfish and microbes in a jellyfish dominated fjord. *Mar. Ecol. Prog. Ser.*, **325**, 29–42.

Smith, D. C. and Azam, F. (1992) Simple, economical method for measuring bacterial protein synthesis rates in seawater using ^{3}H-leucine. *Mar. Microb. Food Webs*, **6**, 107–114.

Sørnes, T. A. and Aksnes, D. L. (2004) Predation efficiency in visual and tactile planktivores. *Limnol. Oceanogr.*, **49**, 69–75.

Steemann Nielsen, E. (1952) The use of radioactive carbon (^{14}C) for measuring organic production in the sea. *J. Cons. Int. Explor. Mer.*, **18**, 117–140.

Stibor, H., Vadstein, O., Diehl, S., Gelzleichter, A., Hansen, T., Hantzsche, F., Katechakis, A., Lippert, B. *et al.* (2004) Copepods act as a switch between alternative trophic cascades in marine pelagic food webs. *Ecol. Lett.*, **7**, 321–328.

Tinta, T., Kogovsek, T., Malej, A. and Turk, V. (2012) Jellyfish modulate bacterial dynamic and community structure. *PLoS One*, **7**, e39274.

Tinta, T., Malej, A., Kos, M. and Turk, V. (2010) Degradation of the Adriatic medusa *Aurelia* sp. by ambient bacteria. *Hydrobiologia*, **645**, 179–191.

Titelman, J., Gandon, L., Goarant, A. and Nilsen, T. (2007) Intraguild predatory interactions between the jellyfish *Cyanea capillata* and *Aurelia aurita*. *Mar. Biol.*, **152**, 745–756.

Titelman, J., Riemann, L., Sornes, T. A., Nilsen, T., Griekspoor, P. and Bamstedt, U. (2006) Turnover of dead jellyfish: stimulation and retardation of microbial activity. *Mar. Ecol. Prog. Ser.*, **325**, 43–58.

Tuomi, P., Fagerbakke, K. M., Bratbak, G. and Heldal, M. (1995) Nutritional enrichment of a microbial community: The effects on activity, elemental composition, community structure and virus production. *FEMS Microbiol. Ecol.*, **16**, 123–134.

Utermöhl, H. (1958) Zur Vervollkommnung der quantitativen Phytoplankton-Methodik. *Mitt. Int. Ver. Limnol.*, **9**, 1–38.

Verity, P. G. and Smetacek, V. (1996) Organism life cycles, predation, and the structure of marine pelagic ecosystems. *Mar. Ecol. Prog. Ser.*, **130**, 277–293.

West, E., Welsh, D. and Pitt, K. (2009b) Influence of decomposing jellyfish on the sediment oxygen demand and nutrient dynamics. *Hydrobiologia*, **616**, 151–160.

West, E. J., Pitt, K. A., Welsh, D. T., Koop, K. and Rissik, D. (2009a) Top-down and bottom-up influences of jellyfish on primary productivity and planktonic assemblages. *Limnol. Oceanogr.*, **54**, 2058–2071.

Wood, S. N. (2011) Fast stable restricted maximum likelihood and marginal likelihood estimation of semiparametric generalized linear models. *J. R. Stat. Soc. Ser. B Stat. Methodol.*, **73**, 3–36.

Zuur, A. F., Ieno, E. N., Walker, N. J., Saveliev, A. A. and Smith, G. M. (2009) *Mixed Effects Models and Extensions in Ecology with R*. Springer, New York.